Desynchronization and synchronization processes in a randomly coupled ensemble of neurons

Vladimir E. Bondarenko[1] and Teresa Ree Chay[2]
[1]*Institute of Biochemical Physics, Russian Academy of Sciences, Kosygin Street 4, Moscow 117334, Russia*
[2]*Department of Biological Sciences, University of Pittsburgh, Pittsburgh, Pennsylvania 15260*
(Received 11 June 1998)

Experimental investigations of the brain shows that synchronization processes play an important role in brain functioning. To simulate this phenomenon we connect 100 model neurons randomly and study the influence of three types of connections (excitatory, inhibitory, and mixed excitatory and inhibitory connections) on the neural network activity. It is found that the neural network model produces a variety of rhythms (from about 2.1 Hz to 180 Hz). The type of activity depends on an injected current, connection strength, and degree of excitability. [S1063-651X(98)10611-6]

PACS number(s): 87.10.+e, 05.45.+b

Systems of coupled oscillators have attracted a great deal of attention for the past two decades because they appear in many physical, chemical, and biological systems (see, for example, [1] and references therein). Specifically, the achievements in this branch of cross-disciplinary science can be applied to the field of neuroscience.

Experimental investigation of the brain shows that a variety of rhythms can be generated by neural ensembles. For example, spindle oscillations (7–14 Hz) and slow oscillations (0.5–4 Hz) are found in the thalamic nucleus [2]. Fast spontaneous oscillations (20–50 Hz) are also present in neocortical and thalamic neurons during wake and sleep states [3]. Jahnsen and Llinás [4] showed that thalamic neurons can produce oscillations in the broad range of frequencies from 10 Hz to 350 Hz, depending on the value of injected current.

Traditionally it is believed that the closer the neurons are in the brain, the more synchronous their activity becomes. On the contrary, recent experiments show that synchronization of neurons in the brain occurs even though they are far from each other [5,6]. This finding requires a revision of the view of the brain and the consideration of the brain as a strongly nonlinear dynamical system, with the network properties being of primary importance.

One more brain property, which can be explained from at least two points of view, is the mechanism of the generation of the rhythms. First, the frequency of the brain's rhythm can be determined by the endogenous frequency of the specific neuron in the definite brain area [7]. Another explanation is that the frequency of the brain's rhythm is determined by the neuron ensemble as a whole system [8].

Previous work [9] was devoted to the study of global synchronization in an ensemble of Hindmarsh-Rose model neurons [10]. It was found that chaos generated by this large neural network can be correlated over large spatial scales. The Hindmarsh-Rose model is based on three differential equations that have little basis in physiology other than the model giving rise to bursting that resembles neuronal bursting. The bursting generated by the neurons in the brain, however, is due to the movement of ions via the ion channels in the plasma membrane. How the ion channel activity can affect the endogenous rhythm and synchronization is of interest in brain research.

This paper is an extension of Ref. [9] with a more realistic neural network with Chay's neurons [11]. We show that this model can produce a variety of rhythms, from slow oscillations (about 2.1 Hz) to very high frequencies (up to 180 Hz), and chaos. The type of activity depends on the value of injected current, connectivity strength, and degree of excitability of the neural network model. This neural network exhibits both synchronous and asynchronous activity at the different time scales: the bursting scale and spiking scale.

The neural network under consideration is described by

$$C_m \frac{dV_i}{dt} = \bar{g}_I m_\infty^3 h_\infty (V_I - V_i) + \bar{g}_{K,V} n_i^4 (V_K - V_i) + \bar{g}_{K,C} \frac{C_i}{1+C_i} (V_K - V_i) + \bar{g}_L (V_L - V_i) + I_{app} + \sum_{j=1, j\neq i}^{N} \bar{a}_{ij} S_j(t), \tag{1}$$

$$dn_i/dt = (n_\infty - n_i)/\tau_n, \tag{2}$$

$$dC_i/dt = \rho m_\infty^3 h_\infty (V_I - V_i) - k_C C_i, \tag{3}$$

where C_m is the membrane capacitance; V_i is the membrane potential of the ith neuron ($i=1,2,\ldots,N$); N is the number of neurons; V_I, V_K, and V_L are the reversal potentials for ''mixed'' Na^+-Ca^{2+}, K^+, and leakage ions, respectively; C_i is the concentration of intracellular Ca^{2+} ions divided by its dissociation constant from the receptor; $\bar{g}_I$, $\bar{g}_{K,V}$, $\bar{g}_{K,C}$, and $\bar{g}_L$ are the maximal conductances; m_∞ and h_∞ are the probabilities of activation and inactivation of the mixed channel; n_i is the probability of opening the voltage-sensitive K^+ channel; n_∞ is the steady state value of n_i; τ_n is the relaxation time; k_C is the rate constant for the efflux of intracellular Ca^{2+} ions; ρ is a factor that converts electrical gradient to chemical gradient while taking care of the surface to the volume ratio; and I_{app} is the injected current. The coupling coefficients $\bar{a}_{ij} = c a_{ij}/N$ are chosen from a uniform random number generator in the interval $[-c/N, c/N]$, where c mea-

sures the synaptic strength. The steady state probability functions m_∞, h_∞, and n_∞ and the relaxation time τ_n are defined by the expressions [11]

$$y=\alpha_y/(\alpha_y+\beta_y),$$

where y stands for m_∞, h_∞, and n_∞, and

$$\alpha_m=0.1(25.0+V)/[1-\exp(-0.1V-2.5)],$$

$$\beta_m=4.0\ \exp[-(V+50.0)/18.0],$$

$$\alpha_h=0.07\ \exp(-0.05V-2.5),$$

$$\beta_h=1/[1+\exp(0.1V-2.0)],$$

$$\alpha_n=0.01(20.0+V)/[1-\exp(-0.1V-2.0)],$$

$$\beta_n=0.125\ \exp[-(V+30.0)/80.0],$$

$$\tau_n=[9.2(\alpha_n+\beta_n)]^{-1}.$$

The ith neuron is connected ''synaptically'' to the jth neuron only when the jth neuron is ''active'' [9]. The activity of jth neuron is denoted by the binary Heaviside function $S_j(t)$, with the threshold potential $V_{th}=-30$ mV. When the jth neuron is active ($V_j>V_{th}$), $S_j(t)=1$; otherwise, $S_j(t)=0$.

Specifically, we investigated the bifurcation structure of an isolated neural cell as a function of the injected current I_{app} [Fig. 1(a)]. When $I_{app}<-2.40\ \mu$A/cm^2 the cell is quiescent. Above this point, we have periodic bursting with two spikes per burst and burst frequency (F_b) from 2.1 to 3.4 Hz. When $I_{app}>-2.08\ \mu$A/cm^2, we have periodic bursting with three spikes per burst and $F_b=2.8$–7.1 Hz. If I_{app} is above $-0.69\ \mu$A/cm^2, we have four spikes per burst and burst frequency of $F_b=5.5$–7.9 Hz. This frequency belongs to the upper θ and spindle regions (7–14 Hz). When $I_{app}=0.04$–$0.12\ \mu$A/cm^2 we have chaotic bursting. A further increase of I_{app} from 0.12 to $0.36\ \mu$A/cm^2 gives periodic bursting again, with five spikes per burst and frequencies of $F_b=6.7$–7.3 Hz. Then, at $I_{app}=0.36$–$0.49\ \mu$A/cm^2, we have chaotic bursting, which leads to an inverse periodic doubling scenario. So, at $I_{app}=0.5\ \mu$A/cm^2, the total length of four different interspike periods is equal to 107 ms, which corresponds to the frequency 9.3 Hz. When $I_{app}=0.53$–$0.63\ \mu$A/cm^2, we have two-spike periods, with a total length of 51–54 ms, which corresponds to the frequencies 18.5–19.6 Hz. Above $I_{app}=0.63\ \mu$A/cm^2, the isolated cell model produces continuous spiking activities, with the spike frequencies from 40 to 101 Hz. Time series of the action potential for different parts of the bifurcation diagram in Fig. 1(a) are shown in Fig. 1(b).

We also investigated the bifurcation structure and two-dimensional (2D) plots of the neurons' activity for the neural network as a function of the type of neuron connectivity: excitatory, inhibitory, and mixed excitatory and inhibitory connections. In the latter case we used approximately equal numbers of excitatory and inhibitory connections. One hundred cells are chosen for our study ($N=100$). In all simulations we used identical initial conditions for all neurons and $I_{app}=0.08\ \mu$A/cm^2 (the case of chaotic bursting of the individual neurons without connections). These initial conditions can be considered as the external stimulus for the neural ensemble.

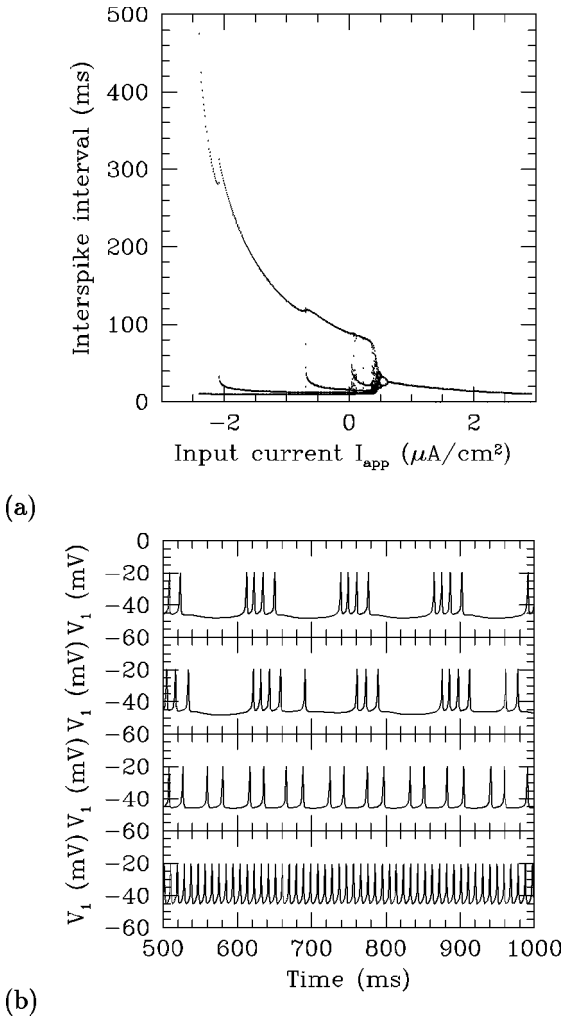

FIG. 1. (a) Bifurcation diagram for the interspike interval vs the injected current I_{app} for an isolated neural cell. (b) Time series of action potential V_1 for increasing values of I_{app} (from top to bottom $I_{app}=0.0$, 0.08, 0.5, and $3.0\ \mu$A/cm^2, respectively). The values of the parameters used in this figure and the subsequent figures are $C_m=1\ \mu$F/cm^2, $V_I=100$ mV, $V_K=-75$ mV, $V_L=-40$ mV, $\bar{g}_I=72.0$ mS/cm^2, $\bar{g}_{K,V}=68.0$ mS/cm^2, $\bar{g}_{K,C}=0.48$ mS/cm^2, $\bar{g}_L=0.28$ mS/cm^2, $\rho=0.0108\ \mu$M/(mV ms), and $k_C=0.001\,94$ ms^{-1}.

At $I_{app}=0.08\ \mu$A/cm^2 and $\bar{a}_{ij}=0.0$ for all i and j ($c=0.0$), we have chaotic synchronous bursting (Fig. 2, second trace). In this case we have independent neurons without connections with identical initial conditions. At $c=3.0$ and $0<a_{ij}<1\ \mu$A/cm^2 (only excitatory connections), the neural network produces regular bursting with four to six spikes and $F_b=6.5$–7.1 Hz. [In neurons there are γ-aminobutyric acid (GABA) secreting inhibitory cells and α-amino-3-hydroxy-5-methyl-4-isoxazdepropionic acid (AMPA) secreting excitatory cells. GABA can ''excite'' Cl^- or K^+ currents, which are outward currents. AMPA, on the other hand, excites a Na^+ current, which is an inward current. We have conceptually modeled this synaptic effect by introducing positive or negative coupling constants.] We observe weak desynchro-

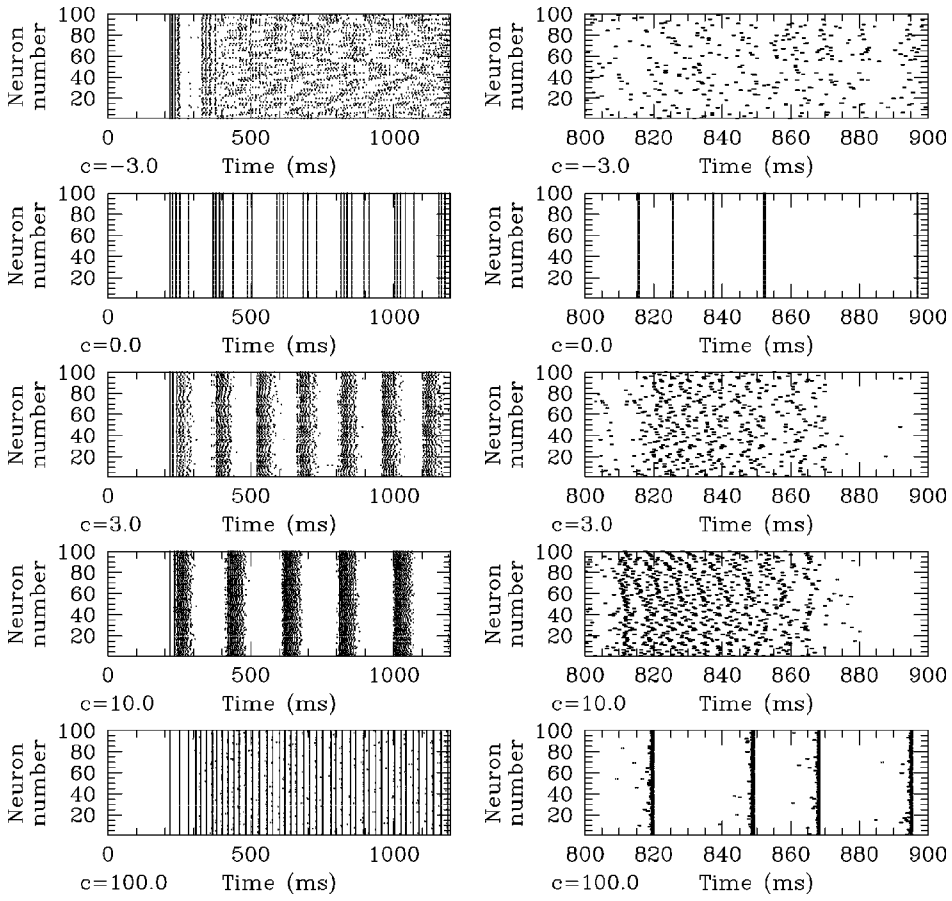

FIG. 2. Two-dimensional plots of the neural network activity with purely inhibitory or purely excitatory connections for different values of strength c. The neuron number is shown on the Y axis. The right column shows the details of the corresponding traces of the left column.

nization of bursts within 20 ms and spiking frequencies of 45–127 Hz (Fig. 2, third trace). Within the burst, chaotic wavelike spiking activity is also found. An increase of c to 10.0 (fourth trace in Fig. 2) gives a decrease of bursting frequency to $F_b=5.1$ Hz, an increase of the number of spikes per burst to 8–9, and an average spiking frequency up to $F_s=180$ Hz. Wavelike spiking activity within the burst becomes more synchronous. A further increase of c to 100.0 (bottom trace in Fig. 2) leads to chaotic spiking activity without bursts, with interspike intervals in the range 18.9–29.4 ms (53–34 Hz). The remarkable property of this regime is that almost all neurons are strongly synchronized (desynchronization is less than 0.25 ms). Thus we see that the increase of connectivity strength and the degree of excitability of the neural network (due to the increase of the average value of excitatory connections) lead to the synchronization of neuron outputs on the level of bursts and spikes. When we used only inhibitory connections in the network at $c=-3.0$ and $0<a_{ij}<1$ μA/cm^2 (upper trace in Fig. 2), we observe another type of activity (chaotic asynchronous bursting or wavelike bursting activity). The transition time from the initial state to this activity is about 200 ms. It corresponds to the reaction time of the neural network to the external stimulus. Note that a further increase of inhibitory connectivity results in only a decrease of the reaction time to about 30 ms at $c=-100.0$, but does not influence qualitatively the 2D picture of the neurons' activity. Thus the inhibitory connections

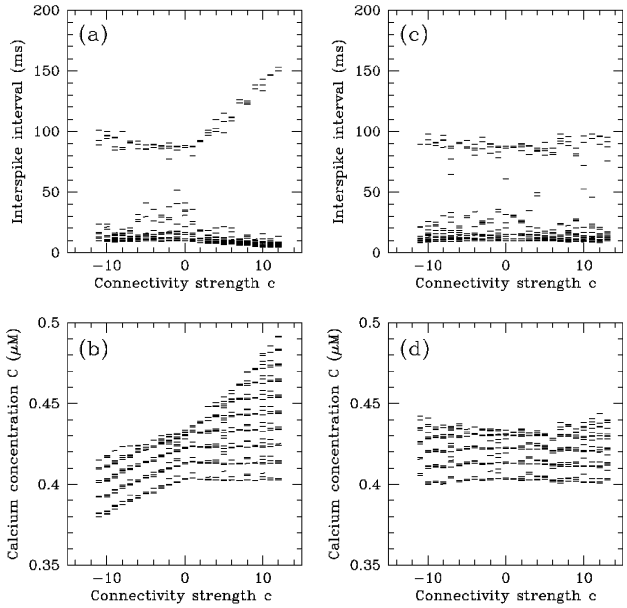

FIG. 3. Bifurcation diagram for (a) and (c) interspike intervals and (b) and (d) calcium concentration vs the connectivity strength c for the first neuron in the network of $N=100$ neurons. We have (a) and (b) only excitatory connections at $\overline{a_{ij}}>0$ for all i and j and only inhibitory connections at $\overline{a_{ij}}<0$ and (c) and (d) mixed excitatory and inhibitory connections -1 μA/cm$^2<a_{ij}<1$ μA/cm^2 for all i and j.

are responsible for desynchronization of neural network activity.

To understand the cause of this different behavior of the neural network for the cases of purely excitatory or purely inhibitory connections on the cell level, we study bifurcation diagrams for interspike intervals [Fig. 3(a)] and calcium concentration [Fig. 3(b)] as functions of connectivity strength. We see that the diagrams have qualitatively different behavior, depending on the strength c. For the positive values of c, we observe the appearance of both low-frequency and high-frequency components in neural network activity. This shift of the bursting frequency from the lower α to the θ region is a pure consequence of the network properties of the neural network. The appearance of a high-frequency component allows better synchronization and, as a consequence, an increase of the average activity amplitude. This property of the highly excitable neural ensemble can be considered as the basis of the appearance of epilepsy. Epileptic activity has similar features: an increase of amplitude, an increase of synchronization, a decrease of chaos, and the appearance of low-frequency components. The analysis of the bifurcation diagram for calcium concentration shows the existence of a stable lower boundary and quantization of C. The increase of connectivity strength yields an increase in the number of spikes per burst and in intracellular calcium concentration. When we have only inhibitory connections (i.e., $c<0$,), we observe a relatively stable bifurcation picture for interspike intervals [Fig. 3(a)]. The behavior of calcium concentration [Fig. 3(b)] is also different from that in the case of purely excitatory connections (i.e., $c>0$). For purely inhibitory connections, the calcium concentration decreases with $|c|$. Perhaps this plays a compensatory role for the increase of $|c|$, supporting stable neural network activity.

We also investigated a bifurcation structure of the neural network model for mixed excitatory and inhibitory connections, with approximately equal numbers of excitatory and inhibitory connections. Bifurcation diagrams for interspike intervals and calcium concentrations are shown in Figs. 3(c) and 3(d), respectively. We see that both figures demonstrate the weak dependence on the connectivity strength. This situation supports the point of view that both excitatory and inhibitory connections are necessary for the stability of neural network functioning (see also [12,13]). Balanced excitatory and inhibitory connections allow us to avoid large calcium fluxes from one cell to another, which are necessary for the production of different functional states.

Thus we show that our neural network model produces a variety of rhythms, from slow oscillations (about 2.1 Hz) to very high frequencies (up to 180 Hz), and chaos. The type of activity depends on the value of the injected current, connectivity strength, and degree of excitability of the neural network model. All these rhythms have been found experimentally in the brain. Our simulations also demonstrate that the excitatory synapses tend to synchronize the neural network activity on the levels of bursts and spikes. An increase of the neural network excitability can lead to a phenomenon that is similar to epilepsy. Inhibitory synapses support desynchronization of bursting and tend to inhibit overloading and large-amplitude oscillations in the neural ensemble.

The authors would like to acknowledge the support of this research by the NSF under Grant No. MCB-9411244 and the Pittsburgh Supercomputing Center through the NIH Division of Research Resources under Cooperative Agreement No. U41 RR0415.

[1] G. V. Osipov, A. S. Pikovsky, M. G. Rosenblum, and J. Kurths, Phys. Rev. E **55**, 2353 (1997).
[2] M. Steriade, D. A. McCormick, and T. J. Sejnowski, Science **262**, 679 (1993).
[3] F. Amzica, D. Neckelmann, and M. Steriade, Proc. Natl. Acad. Sci. USA **94**, 1985 (1997).
[4] H. Jahnsen and R. Llinás, J. Physiol. (London) **349**, 205 (1984).
[5] M. A. L. Nicolelis, L. A. Baccala, R. C. S. Lin, and J. K. Chapin, Science **268**, 1353 (1995).
[6] M. A. L. Nicolelis, E. E. Fanselow, and A. A. Ghazanfar, Neuron **19**, 219 (1997).
[7] R. R. Llinás, Science **242**, 1654 (1988).
[8] M. Steriade and R. R. Llinás, Physiol. Rev. **68**, 649 (1988).
[9] D. Hansel and H. Sompolinsky, Phys. Rev. Lett. **68**, 718 (1992).
[10] J. L. Hindmarsh and R. M. Rose, Proc. R. Soc. London, Ser. B **221**, 87 (1984).
[11] T. R. Chay, Physica D **16**, 233 (1985).
[12] V. E. Bondarenko, in *The Second International Symposium on Neuroinformatic and Neurocomputers, Rostov-on-Don, Russia, 1995* (IEEE, New York, 1995), p. 108.
[13] C. van Vreeswijk and H. Sompolinsky, Science **274**, 1724 (1996).